

## Cross-field diffusion in corotating interaction regions

Devrie S. Intriligator and George L. Siscoe<sup>1</sup>

Space Plasma Laboratory, Carmel Research Center, Santa Monica, California

**Abstract.** Energetic ions associated with the forward and reverse shocks of corotating interaction regions (CIRs) are commonly observed at places within CIRs that are not magnetically connected to either shock. Examples have been documented with data from Pioneer 10 and 11 and Ulysses. They pose a problem for models that account for these shock-associated, corotating energetic ion populations (CEIPs) in terms of ion energization at the shocks followed by ion propagation along field lines. According to these models, regions magnetically unconnected to a shock should contain no shock-associated ions. Cross-field diffusion has been suggested as a mechanism for populating the shock-unconnected regions of CIRs. Here we quantitatively examine this suggestion. We use the Green's function solution to the convection-diffusion equation applied to idealized CIR geometry, with a source at the reverse shock, to compute the ratio of the ion flux in the heart of a CIR to the flux in the shock-connected part of the CIR and to compare the result with typical ratios observed by the Pioneer spacecraft. The computed ratio for resonant diffusion is many orders of magnitude below the observed ratio. For stochastic field line diffusion, the computed ratio is many orders of magnitude above the observed ratio if a diffusion coefficient appropriate to the free solar wind is used. It agrees with the observed ratio, however, if a reduced diffusion coefficient appropriate to CIRs is used. We conclude that the stochastic field model of cross-field diffusion can account for the presence of energetic ions in regions of CIRs that are magnetically unconnected to shock waves.

### Background and Purpose

Corotating interaction regions (CIRs) in the solar wind accelerate background keV energy ions (including solar wind suprathermal ions and interstellar pickup ions) to MeV energies and distribute them in a characteristic way in space [Barnes and Simpson, 1976; McDonald *et al.*, 1976; Pesses *et al.*, 1979]. We summarize the relevant properties here (for additional descriptions, see Tsurutani *et al.* [1982], Richardson, [1985]; Kunow *et al.*, [1991]).

A CIR separates a preceding slow solar wind stream from a following fast solar wind stream. Beyond a heliocentric distance of about 2 AU, a CIR is usually bounded by forward and reverse shocks, and along its whole length it is usually partitioned near the middle by a stream interface, which separates denser, cooler plasma in the slower, preceding stream from thinner, hotter plasma in the faster, following stream. The stream interface can be said to mark the center of a CIR. CIRs generate energetic ions in a pair of corotating energetic ion populations (CEIPs), a leading CEIP and a trailing CEIP. The peak of the leading CEIP lies near the forward shock, and the peak of the trailing CEIP lies near the reverse shock; the peaks may or may not coincide with the shocks. The trailing CEIP is often more

pronounced than the leading CEIP. The two CEIPs are separated by a valley of low flux in the center of the CIR. A recent finding of direct relevance to this paper is that the stream interface lies at the foot of the slope that leads from the valley floor up to the peak of the trailing CEIP [Intriligator and Siscoe, 1994], (hereinafter referred to as paper 1).

Figure 1 illustrates general CIR morphology with a particular example. The data were taken during Bartel's rotation 1927 in 1974 by Pioneer 11 at a heliocentric distance near 4 AU. They show the jumps in solar wind speed at the forward and reverse shocks, the jump in the specific entropy within the CIR marking the stream interface, and the two peaks in the energetic ion fluxes forming the leading and trailing CEIPs. The stream interface lies at the bottom of the slope up to the trailing CEIP. The asymmetrical shape of the valley seen here is typical: The slope of the valley wall leading down to the stream interface is shallower on the leading side than on the trailing side (Figure 3 of paper 1 gives more examples). This asymmetry cannot be explained in terms of the unequal sizes of the two CEIP peaks, because the shallow slope is distinct from the slope associated with the leading CEIP. Below, we suggest an explanation in terms of a spatially varying diffusion coefficient.

Data of this kind have stimulated efforts to explain the acceleration process that makes CEIPs. Fermi acceleration [Palmer and Gosling, 1978; Fisk and Lee, 1980] seems capable of providing the bulk of the CEIPs, and gradient drift acceleration [Pesses *et al.*, 1979, 1982] might provide local flux peaks near the shocks [Lee, 1983]. Less attention has been paid to how the ions are transported once accelerated. Propagation parallel to the magnetic field has been assumed; transport perpendicular to the field has been mostly ignored.

<sup>1</sup>Also at Center for Space Physics, Boston University, Boston, Massachusetts.

Copyright 1995 by the American Geophysical Union.

Paper number 95JA01916.  
0148-0227/95/95JA-01916\$05.00

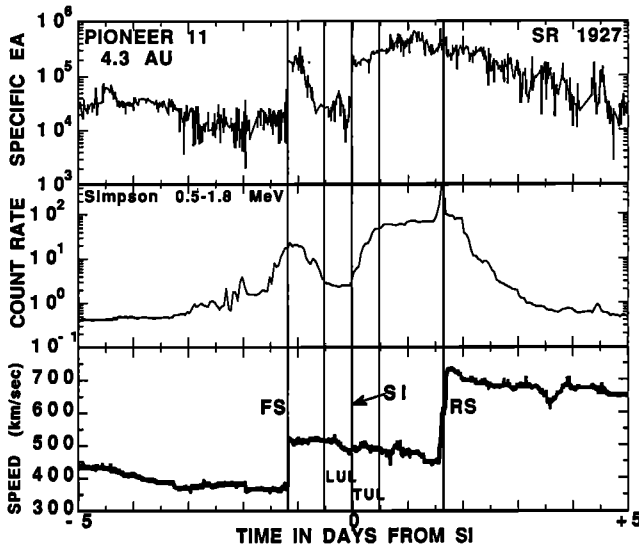


**Figure 1.** Pioneer 11 solar wind specific entropy argument (EA) in units of  $\text{K cm}^{-1/2}$ , corotating energetic ion population (CEIP) profile as seen in Simpson's 0.5-1.8 MeV protons, and solar wind speed for a corotating interaction region (CIR) at 4.3 AU in solar rotation (SR) 1927 in 1974 [Intriligator and Siscoe, 1994]. Marked features are the following: FS, forward shock; SI, stream interface; RS, reverse shock; LUL, leading unshocked layer; TUL, trailing unshocked layer.

Data from the central valley of minimum flux allowed us to examine this aspect of the transport.

Since CEIPs are associated with the shocks, one could have anticipated a central valley of low fluxes, because the shocks do not start at the stream interface within a CIR. A shock's sunward tip comes closest, approaching to within roughly 12 corotation hours of the stream interface [Pizzo, 1989; Hu, 1993]. Figure 1 gives 12-hour markers to show where the tip of the shocks project along field lines to the spacecraft's position. The spaces between the shocks and the stream interface are labelled LUL (leading unshocked layer) and TUL (trailing unshocked layer). Much of the trailing CEIP lies in the TUL. From this perspective, the valley is interesting, not because it has fewer energetic ions, but because it has energetic ions at all. How does a part of a CIR that is magnetically unconnected to a shock receive ions accelerated by a shock?

Tsurutani *et al.* [1982] were first to point out the anomalous presence of energetic ions in the unshocked valleys of CIRs and the first to suggest how they might get there. They described a recurring CIR whose valley partially filled in during a series of recurrences: Its flux went from below ambient near the time of the CIR's appearance to above ambient on later recurrences. They conjectured that the filling in was "presumably due to cross-field diffusion of protons from the neighboring maximum regions" (p. 7389). Gradient drift at the shock cannot fill in the valley since the shocks do not enter the valley. (Tsurutani *et al.* also noted that the energetic ions in the unshocked layers could come from the sun or from greater heliocentric distances.)

In paper 1, we questioned whether the cross-field diffusion mechanism can fully account for the presence of

energetic ions in the central valley in view of the finding, already mentioned, that the stream interface acts as if it were a border to the trailing CEIP. This finding was based on data from Pioneer 10 and 11. It refers to CIRs near the ecliptic plane between about 3 AU and 5 AU. It was subsequently confirmed using Ulysses data on CIRs around 5 AU off the ecliptic plane [Intriligator *et al.*, 1995]. Between the two studies, 12 cases were tested; the result held for each. It put the cross-field diffusion conjecture in question, because the stream interface plays no apparent role in ion diffusion. Nonetheless, we solve the applicable convection-diffusion equation below and show that cross-field diffusion is fast enough to populate the unshocked valley with energetic ions as observed. Indeed, the quantitative treatment of the transport shows that diffusion is too effective, which turns the original question around to, How does the valley stay so empty? The answer to the revised question comes from an earlier work [Conlon, 1978] on the transport of relativistic electrons from Jupiter through the solar wind. This study revealed that cross-field diffusion is strongly suppressed within CIRs. Here we show that the suppression accounts quantitatively for the observed fluxes. In light of the result, the morphological evidence that earlier argued against diffusion, namely, that the stream interface borders the trailing CEIP, must be regarded as requiring a separate explanation from a cross-field diffusion model. We consider this requirement after showing that cross-field diffusion quantitatively accounts for the flux of energetic ions observed in the central valley.

### Green's Function Solution of the Convection-Diffusion Equation for CIR Geometry

Figure 2 gives an idealized geometry for the trailing half of a CIR. The idealization consists in unbending the spirals that describe the actual stream interface and the reverse shock and aligning the coordinate system with the unbent stream interface, field lines, and flow lines in the corotating reference frame. In this geometry, magnetic field lines, between the stream interface and the reverse shock lie parallel to the stream interface. Thus the directions parallel and perpendicular to the magnetic field coincide with the directions of the coordinate axes. The geometry is two dimensional and time stationary. The assumption of two dimensionality is justified, since the unshocked layers are about 0.1 AU thick and several AU in the other two dimensions. The assumption of time independence in the corotating frame is justified, since the diffusion time scale is about 5 days (based on  $k_{\perp} = 2.5 \times 10^{18} \text{ cm}^2 \text{ sec}^{-1}$ ; see below), whereas the valley in the flux profile persisted for nearly a year. The geometry is time-stationary in the corotating reference frame where the solar wind flow is parallel to the magnetic field. These idealizations greatly assist in solving the equation, and the errors they cause are not likely to affect the conclusions based on the results.

The convection-diffusion equation appropriate to the idealized geometry is

$$k_{\perp} \frac{\partial^2 f}{\partial x^2} + k_{11} \frac{\partial^2 f}{\partial y^2} - v \frac{\partial f}{\partial y} = 0 \quad (1)$$

where  $f$  is the omnidirectional distribution function;  $x$  and  $y$

are coordinate directions perpendicular and parallel to the flow and field lines;  $k_{\perp}$  and  $k_{11}$  are coefficients for diffusion perpendicular and parallel to the magnetic field; and  $V$  is solar wind speed in the corotating frame. In the data,  $f$  is proportional to counts per second in a fixed energy range. Conditions are assumed to be constant in the  $z$  direction, that is, perpendicular to the plane of the figure. The adiabatic deceleration term is omitted, but its effect is considered below. The boundary conditions are a delta function source at the shock with arbitrary source strength along the shock and vanishing particle intensities at infinity. We solve the equation by first going into the solar wind reference frame, which transforms the equation into a pure diffusion equation with a moving source. The expression for the moving source can be inserted into the Green's function solution to the time-dependent, two-dimensional diffusion equation [Morse and Feshbach, 1953, p. 894]. Transforming back to the original reference frame then gives

$$f(x,y) = \int_{\text{shock}} S(\xi_0) d\xi_0 \int_0^{\infty} \frac{d\tau}{\tau} \exp \left[ -\frac{(\xi - \xi_0)^2 + (\eta - \mu\xi_0 - \nu\tau)^2}{4\tau} \right] \quad (2)$$

Here  $S(x)$  is the source strength along the shock measured at its  $x$  position;  $\xi = x\sqrt{k_{\perp}}$ ;  $\eta = y\sqrt{k_{11}}$ ;  $\mu = m\sqrt{k_{\perp}/k_{11}}$ , in which  $m$  is the slope of the shock defined by  $y = mx + b$ , where  $b$  is the  $y$  intercept of the shock; and  $\nu = V\sqrt{k_{\perp}}$ . The inner integral is the Green's function for our problem. The Green's function gives the contribution to  $f$  at an arbitrary point  $(x,y)$  from particles generated at an arbitrary point  $x_0$  on the shock surface. We must integrate the Green's function along the shock surface to get the full value of  $f$  at  $x,y$ . The inner integral in equation (2) can be evaluated under an approximation that applies to our case, namely,

$$2\nu\sqrt{(\xi - \xi_0)^2 + (\eta - \mu\xi_0)^2} > 1 \quad (3)$$

One then obtains an approximation for the Green's function,  $g(x,y | x_0)$ :

$$g(x,y | x_0) \cong \sqrt{2\pi} \exp \left[ -\frac{V}{2k_{11}} \left[ \sqrt{\frac{k_{11}}{k_{\perp}}(x-x_0)^2 + (y-mx_0)^2} - (y-mx_0) \right] \right] \div \left[ \frac{V}{2k_{11}} \sqrt{\frac{k_{11}}{k_{\perp}}(x-x_0)^2 + (y-mx_0)^2} \right]^{1/2} \quad (4)$$

With this result, we can formulate a procedure to compare the empirical flux ratio across the unshocked layer with that predicted by equation (2). We could simply integrate equation (2) numerically, but the uncertainty in specifying the source function  $S(x)$  would leave the result open to multiple interpretations. Instead, we take advantage of an analytical property of equation (4). For our standard

of comparison, we take the ratio of intensities at the inner and outer edges of the trailing unshocked layer at a nominal distance of 4 AU, approximately where Pioneer 11 made its measurements. Our representative value for this flux ratio is 1/20. Now equation (4) can be used to show that the part of the shock that gives the biggest contribution to the ratio is the part closest to the stream interface, that is, the sunward tip of the shock. Thus if the ratio based on this part alone is too small, so will be the ratio based on the full integration of all source points along the shock. Our procedure, then, is to calculate ratios of values of  $g(x,y | x_0)$  computed for the two sides of the trailing unshocked layer and to compare the ratios with 1/20. This procedure minimizes the impact of neglecting the adiabatic deceleration term, since the amount of deceleration is nearly the same for ions created at one point on the shock.

It is convenient to take the origin of the  $(x,y)$  coordinate system to be the sunward tip of the shock. Then the  $y$  axis passes through  $x_0$  and the  $x$  position of the outer edge of the trailing unshocked layer. Equation 4 gives for the ratio of the flux at the stream interface to the flux across the unshocked layer from ions generated at the sunward tip of the shock

$$R(k_{11}, k_{\perp}) = \left[ \frac{y_P^2}{\frac{k_{11}}{k_{\perp}} x_{SI}^2 + y_P^2} \right]^{1/4} \exp \left[ \frac{V}{2k_{11}} \left[ y_P - \sqrt{\frac{k_{11}}{k_{\perp}} x_{SI}^2 + y_P^2} \right] \right] \quad (5)$$

in which  $y_P$  is the  $y$  position of the Pioneers relative to the sunward tip of the shock, and  $x_{SI}$  is the  $x$  position of the stream interface. Since  $y_P$ ,  $x_{SI}$ , and  $V$  are known at least approximately, the ratio  $R(k_{\perp}, k_{11})$  can be regarded to be a function of the diffusion coefficients. Numerical MHD models [e.g., Pizzo, 1989; Hu, 1993] and observations agree that the sunward tip of the reverse shock lies typically around 2 AU, which gives  $y_P = 8.3$  AU (the distance along a corotation spiral from 2 AU to 4 AU radial distance). These MHD models also give  $x_{SI}$  equal to a corotation time of about 12 hours in the spacecraft frame, which at 4 AU is about 0.12 AU in the orthospiral direction (that is, perpendicular to the corotation spiral). For  $V$  we take 1500 km/sec (corresponding to a 500 km/s solar wind and a corotation speed based on the midpoint between 2 AU and 4 AU). With these values we can construct contour plots of  $R(k_{11}, k_{\perp})$  for a range of diffusion coefficients. Since  $k_{\perp}$  enters only as a ratio with  $k_{11}$ , we show contour plots of  $R(k_{11}, k_{\perp}/k_{11})$ . Figure 3 summarizes this information.

The contours of the ratio  $R(k_{11}, k_{\perp}/k_{11})$  go from a precipitous  $10^{-5}$  to a flat  $10^{-0.01}$ . The thick contour at  $10^{-1.3}$  ( $= 0.05$ ) corresponds to the characteristic observed ratio, 1/20. For cross-field diffusion to fill in the unshocked layer, to the extent suggested by observations, lines of constant  $k_{11}$  and  $k_{\perp}/k_{11}$  must cross near this thick contour. The shaded region to the right in the figure corresponds to estimates for  $k_{11}$  and  $k_{\perp}/k_{11}$  appropriate to the free solar wind. These are

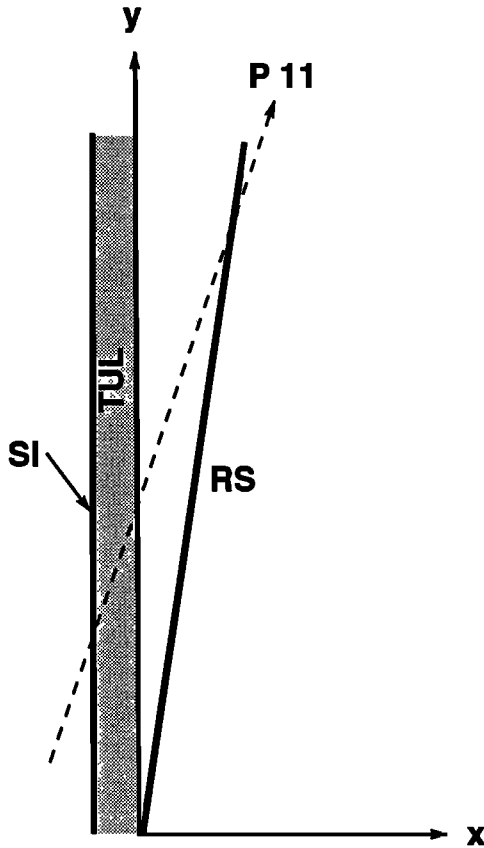


Figure 2. Coordinate system and reference frame in which the convection-diffusion problem is formulated and solved.

taken from the Palmer [1982] survey. They are based on 1 MeV protons and the suggestion by Palmer that over the range 1 AU to 5 AU, the diffusion coefficient is approximately independent of heliocentric distance. The free solar wind range of  $k_{\perp}/k_{11}$  uses none of the estimates for which Palmer gives only upper limits. (Upper limit estimates come mostly from fitting the flux profiles of flare proton events. The identification of similar proton events with CMEs [Kahler, 1993] subsequent to the Palmer survey changes the assumptions on which the estimates are based.) The intersection of the two shaded bands defines the free solar wind domain of flux ratios. It lies wholly in the part of the plot where the flux is greater than observed. This means that if the free solar wind values of  $k_{11}$  and  $k_{\perp}/k_{11}$  also applied inside CIRs, one should never see a valley with a factor of 20 depression; our problem would be to explain why the unshocked layers are so empty instead of why they are partially filled in. The value of  $k_{11}$  or  $k_{\perp}/k_{11}$  or both inside the CIR must be less than their free solar wind values; otherwise, the unshocked layer would fill in more than is observed.

The following argument suggests that the value of  $k_{11}$  does not change much from the free solar wind to a CIR. The ratio of the change is given by equation (6), which is based on an expression derived by Giacalone *et al.* [1993, equation 8].

$$\frac{(k_{11})_{\text{CIR}}}{(k_{11})_{\text{SW}}} = \frac{(B^{\delta})_{\text{CIR}}(P_o)_{\text{SW}}}{(B^{\delta})_{\text{SW}}(P_o)_{\text{CIR}}} \quad (6)$$

Here  $B$  is field strength, and  $P_o$  and  $\delta$  are defined by  $P(k) = P_o k^{-\delta}$ , where  $P(k)$  is the power density at wave number  $k$ . To obtain an average ratio of field strengths, we have used the first nine recurrences of the bigger of the two giant streams of 1974 (the series Tsurutani *et al.* [1982] analyzed). This gives  $9.0 \pm 5.1$ . From many power spectra of field fluctuations near the stream interfaces of these CIRs, we find that the value of  $\delta$  is close to the Kolmogoroff 5/3, which we use. (Equation (6) assumes that  $\delta$  is nearly the same in the free solar wind and in CIRs, as appears to be the case [Ruzmaikin *et al.* 1995].) For the ratio of  $P_o$ s, we use the ratio of the variances of the components, which ranges from 20 to 65. Using 9.0 for the ratio of field strengths and 42 (the median of the range) for the ratio of powers, we find that the ratio of  $k_{11}$ s is essentially unity. The increased amplitude of fluctuations approximately compensates for the increased field strength. Thus in Figure 3, the CIR domain should lie on the Palmer consensus band of  $k_{11}$ s. The problem remains to fix its location along the  $k_{\perp}/k_{11}$  axis.

Since  $k_{11}$  changes little from the free solar wind to the CIR, we can consider change in  $k_{\perp}/k_{11}$  or the change in  $k_{\perp}$ . To get at the change in  $k_{\perp}$ , we look at the two basic cross-field diffusion mechanisms that have been discussed: wave particle (also known as resonant) scattering and the random walk of magnetic field lines (also known as the stochastic field model) [Jokipii, 1966; Jokipii and Parket, 1969]. With regard to resonant scattering, Palmer [1982] notes that for ions with energies around 1 MeV in the free solar wind, cross-field diffusion by this mechanism is "all but negligible." To see that it is also negligible in CIRs, consider the following resonant scattering formula [Jokipii, 1987, equation (5)]:

$$\frac{k_{\perp}}{k_{11}} = \frac{1}{1 + (\lambda_{11}/r_g)^2} \quad (7)$$

Here  $\lambda_{11}$  is the parallel mean free path and  $r_g$  is the ion gyroradius. Palmer gives the range 0.08 AU to 0.3 AU for  $\lambda_{11}$  in the free solar wind, which we have argued applies also to CIRs. The average CIR field strength measured by Pioneer 11 (3.7 nT) gives  $2.5 \times 10^{-4}$  AU for the gyroradius of a 1 - MeV proton. These numbers give  $7 \times 10^{-7}$  to  $1 \times 10^{-5}$  for the range of  $k_{\perp}/k_{11}$ , which lies well to the left of the border of Figure 3. Thus resonant scattering can be neglected within CIRs as well as in the free solar wind.

This leaves the stochastic field model. To apply it to estimate how much  $k_{\perp}$  changes from the free solar wind to CIRs, we adopt an idea put forth by Conlon [1978]. Conlon analyzed Pioneer 11 data to determine the manner in which relativistic electrons escaping from Jupiter's magnetosphere propagate through the solar wind. They readily filled the volume occupied by a free solar wind stream, from which Conlon deduced that cross-field diffusion in the free solar wind must be as rapid as the stochastic field model allows. He observed, however, that the flux of relativistic Jovian electrons was greatly reduced in CIRs, which implied a correspondingly reduced value of  $k_{\perp}$ . To account for a small  $k_{\perp}$ , he reasoned that a CIR's spirallike corotating shocks compress the average, spiral part of the field more than the fluctuating, random walking part of the field, or at least that component that fluctuates parallel to the shock

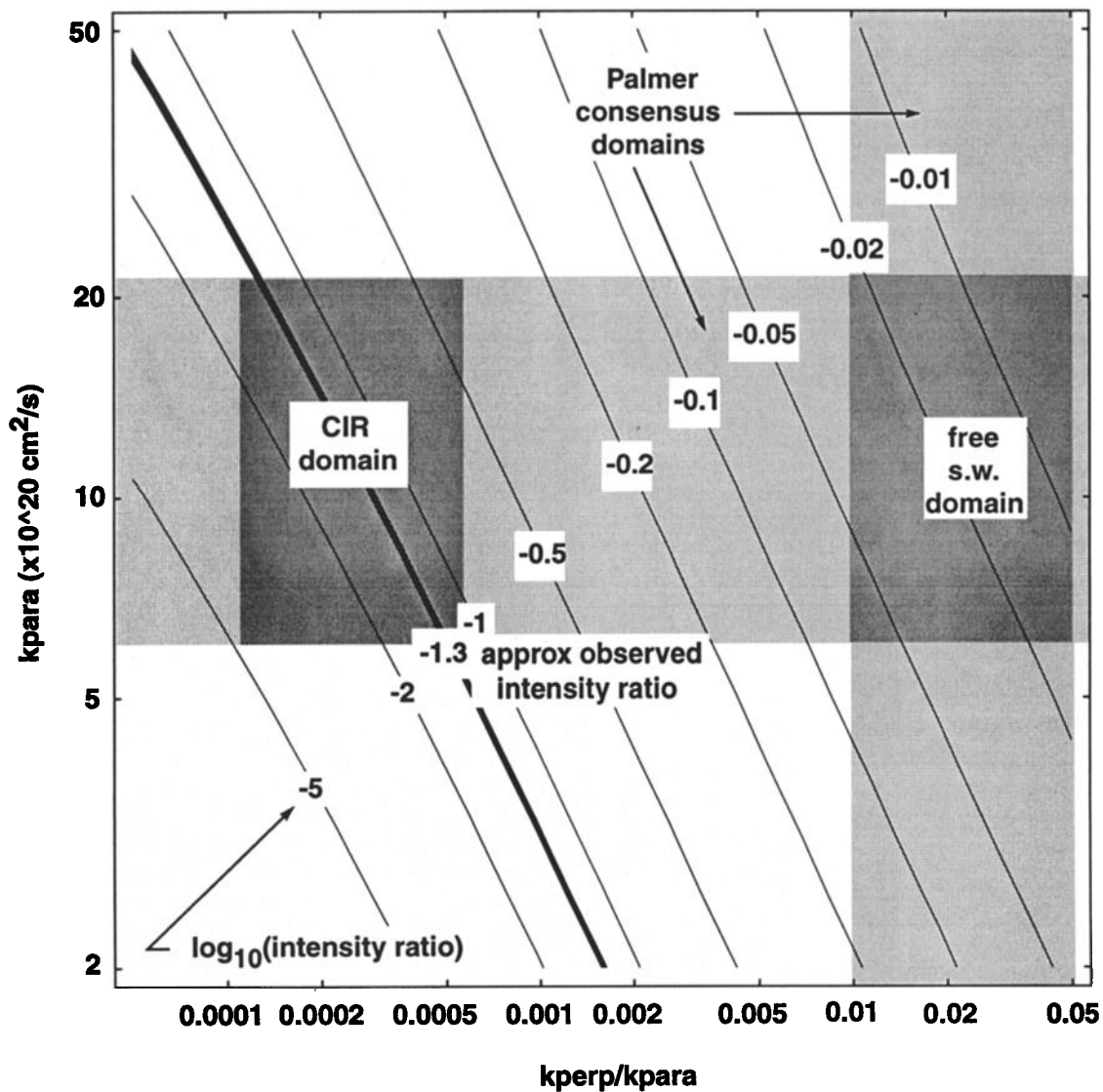


Figure 3. Contours of the ratio of the flux at the stream interface to the flux just across the unshocked layer as a function of  $k_{\perp}$  and  $k_{\perp}/k_{\parallel}$ . The thick contour represents the observed ratio. The heavily shaded regions identify the parameter regimes for the diffusion coefficients that are characteristic of the free solar wind and the CIRs.

normal, which is the uncompressed component. Strengthening the average field but not the cross-field fluctuations straightens the kinks in the field lines that are responsible for random walking the field across the CIR, thus reducing the cross-field diffusion coefficient. Stated differently, shock compression does not increase the amount of field line tangling, it merely compresses the preexisting tangled mass like a ball of steel wool. This analogy captures the idea of reversible compression of a dense network of lines, though not the aspect that the lines form a rope. In this view, whereas before the compression occurred, a particle might move along a tangled field line a distance  $x$  across the average field direction while moving a distance  $y$  along the average direction, after compression, a particle following the same field line would move only a distance  $x/c$  across the average field direction while moving the same distance  $y$  along the average direction, where  $c$  is the compression ratio (the ratio of the CIR field strength to the free solar wind

field strength). Since diffusion is a random walk process, the cross-field motion enters the diffusion coefficient squared; hence the diffusion coefficient in a CIR goes down by the square of the compression ratio. For our Pioneer CIR sample, this gives about a factor of 80 reduction in  $k_{\perp}$ , which is the factor used to locate the CIR domain in Figure 3. (Conlon inferred a factor of 1600, but this was based on the weakest solar wind field strength. We have used the field strength just upstream from the reverse shock, since this is the field on which our estimate on  $k_{\perp}$  in the CIR is based.)

Though the shock is not a tangling mechanism, it does increase the level of fluctuations, as *Tsurutani et al.* [1982] show. They also show that the added fluctuations are mainly Alfvénic, since the field strength fluctuates little. This type of fluctuation propagates along the average field direction and contributes inefficiently, if at all, to stretching the tangled field perpendicular to the average field direction.

Thus while the added fluctuations act to decrease  $k_{11}$  significantly, as equation (6) shows (but the compressed field strength acts to increase it again to about its free solar wind value), they do little to  $k_{\perp}$ . The whole effect on  $k_{\perp}$  results simply from squashing the field line tangle in the cross-CIR direction, with a corresponding shrinking of the mean-free path in that direction. This dramatically weakens the flux of relativistic electrons in CIRs as *Conlon* [1978] observed, and it centers the CIR domain in Figure 3 on the reference contour representing the observed flux ratios. (We acknowledge that a recent interpretation by *Bieber et al.* [1994] would put the Palmer band about a factor of 2 lower than the original; but even if the *Bieber et al.* interpretation proves to be correct, it will not change our results, owing to the fact that the reference contour line passes through the CIR domain.)

We conclude that the stochastic field model can account for the 5% of the shock-fed flux of energetic ions that cross the unshocked layer to reach the stream interface at 4 AU. The question remains, Why does it stop there? The next section addresses this and a related question.

### Requirements on the Cross-field Diffusion Explanation Imposed by Morphology

In the equations of diffusive transport, the determining elements are the diffusion coefficient and the sources and sinks of particles; nothing else enters. Thus in general terms, if the stream interface is to play a role in determining the spatial distribution of ions under diffusive transport, it must be a source, a sink, or a separator of regions having different diffusion coefficients. It cannot be a source, because the flux falls to a minimum there. It might, however, act as a sink in a time-dependent situation where the level of the valley rises by the diffusive influx of ions from both sides, as *Tsurutani et al.* [1982] suggested. Yet even here the coincidence between the stream interface and the low point in the valley is not guaranteed, since the unshocked region defining the valley is much wider than the stream interface; the valley's low point could be anywhere, not necessarily at the stream interface. Some extra piece of physics presumably connects the two features; otherwise, if the physics that governs the stream interface were completely independent of the physics that governs the CEIPs, a near coincidence between the stream interface and the valley's low point would not occur in most of the 12 observed cases. We have mentioned that MHD models of CIRs indicate that the forward and reverse shocks form about equidistant from the stream interface, but this is insufficient as an explanation, because in a purely diffusive situation, the valley's low point falls where the opposing diffusive fluxes balance, not where the opposing distances balance. For example, other things being equal, the low point should lie closer to the weaker source; yet no reason is known for the location of the stream interface similarly to depend on the relative strengths of the sources. If the stream interface had no influence on the diffusion, our null hypothesis, the flux from the stronger source would simply diffuse through the stream interface to get to the low point. Therefore some factor must operate to lock the stream interface into the valley's low point.

It is possible that the stream interface is indeed a physical barrier to stochastic field diffusion. Perhaps field lines have not random walked across it near the Sun and cannot random walk across it farther out. This possibility would be consistent with the stream interface being a tangential discontinuity. A tangential discontinuity separates plasma with different histories. Thus any random walking across a tangential discontinuity would have to occur after the plasmas had met and the tangential discontinuity had formed. But fields can be strongly sheered across a tangential discontinuity, which would inhibit field lines from one side invading the other side. Furthermore, the stream interface is relatively thin, which implies a suppression of diffusive processes, such as stochastic field diffusion, that would act to thicken it. More generally, a tangential discontinuity is a field line surface, which means that once it is formed, fields lines neither enter nor leave it. Therefore field lines from one side do not cross it to mix with field lines on the other side.

What evidence is there that the stream interface is a tangential discontinuity? There is the direct evidence that the plasma temperature is discontinuous at the stream interface. In some CIRs, the temperature jumps an order of magnitude in less than an hour. There is the indirect evidence that the stream interface has been observed to lie within one corotation hour of the heliospheric current sheet from 1 AU to 5 AU [*Siscoe and Intriligator*, 1994]. The heliospheric current sheet is a tangential discontinuity [*Klein and Burlaga*, 1980]. As *Siscoe and Intriligator* [1994] argued, this implies that the stream interface is also a tangential discontinuity. The proximity of the stream interface and the heliospheric current sheet puts an upper limit of  $10^{-4}$  nT on the difference in the normal components of the fields at their surfaces. A good assumption is that the normal components are zero in both cases and that both are tangential discontinuities.

As noted earlier, the flux varies asymmetrically between CEIP peaks. Its slope is much shallower before the stream interface than after it. In a diffusion scenario, this means that the stream interface separates regions having different diffusion coefficients, the preceding coefficient being bigger. This is a significant result of the present analysis. It says that the degree of field line tangling in the plasma that precedes the stream interface is significantly greater than the degree of field line tangling in the plasma following. The plasma feature that precedes the stream interface is presumably the streamer belt [cf. *Gosling et al.*, 1981, Figure 8]. Therefore we infer that field lines inside the streamer belt are more stochastic than field lines outside. There is indirect support for this inference. *Crooker et al.* [1993] and *Nakagawa* [1993] find marked deviations from corotating spiral geometry to characterize the magnetic field in the streamer belt.

### Summary

This study has yielded two main results: (1) The energetic ions in the central shock-unconnected region of CIRs can arrive there by stochastic cross field-diffusion from shock-connected parts of the CIR and (2) to account for the relatively few ions in the central region, the stochastic field diffusion coefficient must be reduced by nearly 2 orders of

magnitude from its free solar wind value, corresponding to the ratio of field strengths inside and outside the CIR as suggested by Conlon [1978]. These conclusions supersede the suggestion by *Intriligator and Siscoe* [1994] that some nondiffusive mechanism populates the central region with energetic ions. In the present paper, the reasons for the earlier suggestion take the form of requirements on the diffusion scenario. There are two requirements: (1) The stream interface must act like a physical barrier to the stochastic field diffusion of ions generated by the reverse shock (an attribute it might acquire by being a tangential discontinuity) and (2) the coefficient of stochastic field diffusion must be much greater before the stream interface than after it or, stated differently, field lines must be more stochastic inside the streamer belt than outside (a condition for which there is independent evidence).

**Acknowledgments.** We are grateful to the Pioneer Project Office for the continued success of the Pioneer missions. We are indebted to E. J. Smith and A. Barnes, F. B. McDonald and J. A. Simpson, and J. A. Van Allen for generously making available the magnetic field, plasma, and energetic particle data, respectively. We also are indebted to Don Ellison, Jack Gosling, Phil Isenberg, Randy Jokipii, Marti Lee, Bill Webber, and Gerd Wibberenz for discussions of this work. This work was supported by NASA Ames Research Center under contract NAS2-13692 and by Carmel Research Center.

The Editor thanks I. G. Richardson and A. A. Ruzmaikin for their assistance in evaluating this paper.

## References

- Barnes, C.W., and J.A. Simpson, Evidence for interplanetary acceleration of nucleons in corotating interaction regions, *Astrophys. J.*, *210*, L91-L96, 1976.
- Bieber, J.W., W.H. Matthaeus, C.W. Smith, W. Wanner, M.-B. Kallenrode, and G. Wibberenz, Proton and electron mean free path: The Palmer consensus revisited, *Astrophys. J.*, *420*, 294, 1994.
- Conlon, T.F., The interplanetary modulation and transport of Jovian electrons, *J. Geophys. Res.*, *83*, 541-552, 1978.
- Crooker, N.U., G.L. Siscoe, S. Shodhan, D.F. Webb, J.T. Gosling, and E.J. Smith, Multiple heliospheric current sheets and coronal streamer belt dynamics, *J. Geophys. Res.*, *98*, 9371-9381, 1993.
- Fisk, L.A., and M.A. Lee, Shock acceleration of energetic particles in corotating interaction regions in the solar wind, *Astrophys. J.*, *237*, 620-626, 1980.
- Giacalone, J., D. Burgess, S.J. Schwartz, and D.C. Ellison, Ion injection and acceleration at parallel shocks: Comparisons of self-consistent plasma simulations with existing theories, *Astrophys. J.*, *402*, 550-559, 1993.
- Gosling, J.T., G. Borrini, J.R. Asbridge, S.J. Bame, W.C. Feldman, and R.T. Hansen, Coronal streamers in the solar wind at 1 AU, *J. Geophys. Res.*, *86*, 5438-5448, 1981.
- Hu, Y.Q., Evolution of corotating stream structures in the heliospheric equatorial plane, *J. Geophys. Res.*, *98*, 13,201-13,214, 1993.
- Intriligator, D.S., and G.L. Siscoe, Stream interfaces and energetic ions closer than expected: Analyses of Pioneer 10 and 11 observations, *Geophys. Res. Lett.*, *21*, 1117-1120, 1994.
- Intriligator, D.S., G.L. Siscoe, G. Wibberenz, H. Kunow, and J.T. Gosling, Stream interfaces and energetic ions 2, Ulysses test of Pioneer results, *Geophys. Res. Lett.*, *22*, 1173-1176, 1995.
- Jokipii, J.R., Cosmic ray propagation, 1, Charged particles in a random magnetic field, *Astrophys. J.*, *146*, 480, 1966.
- Jokipii, J.R., Rate of energy gain and maximum energy in diffusive shock acceleration, *Astrophys. J.*, *313*, 842-846, 1987.
- Jokipii, J.R., and E.N. Parker, Stochastic aspects of magnetic lines of force with application to cosmic-ray propagation, *Astrophys. J.*, *155*, 177, 1969.
- Kahler, S.W., Coronal mass ejections and long rise times of solar energetic particle events, *J. Geophys. Res.*, *98*, 5607-5615, 1993.
- Klein, L., and L. Burlaga, Interplanetary sector boundaries, 1971-1973, *J. Geophys. Res.*, *85*, 2269-2276, 1980.
- Kunow, H., G. Wibberenz, G. Green., R. Müller-Mellin, M. Witte, H. Hempe, R.A. Mewaldt, E.C. Stone, and R.E. Vogt, Simultaneous observations of cosmic ray particles in a corotating interplanetary structure at different solar distances between 0.3 and 1 AU from Helios 1 and 2 and IMP 7 and 8, *Proc. Int. Conf. Cosmic Rays*, *3*, 227, 1991.
- Lee, M.A., Coupled hydromagnetic wave excitation and ion acceleration at interplanetary traveling shocks, *J. Geophys. Res.*, *88*, 6109-6119, 1983.
- McDonald, F.B., B.J. Teegarden, J.H. Trainor, T.T. von Rosenvinge, and W.R. Webber, The acceleration of energetic ions, *Astrophys. J. Lett.*, *203*, L149, 1976.
- Morse, P.M., and H. Feshbach, *Methods of Theoretical Physics*, McGraw-Hill, New York, 1953.
- Nakagawa, T., Solar source of the interplanetary magnetic structures, *Sol. Phys.*, *147*, 169-197, 1993.
- Palmer, I.D., Transport coefficients of low-energy cosmic rays in interplanetary space, *Rev. Geophys.*, *20*, 335-351, 1982.
- Palmer, I.D., and J.T. Gosling, Shock-associated energetic proton events at large heliocentric distances, *J. Geophys. Res.*, *83*, 2037-2046, 1978.
- Pesses, M.E., B.T. Tsurutani, J.A. Van Allen, and E.J. Smith, Acceleration of energetic protons by interplanetary shocks, *J. Geophys. Res.*, *84*, 7297-7301, 1979.
- Pesses, M.E., R.B. Decker, and T.P. Armstrong, Acceleration of charged particles in interplanetary shock waves, *Space Sci. Rev.*, *32*, 185, 1982.
- Pizzo, V.J., The evolution of corotating stream fronts near the ecliptic plane in the inner solar system, 1, Two-dimensional fronts, *J. Geophys. Res.*, *94*, 8673-8684, 1989.
- Richardson, I.G., Low energy ions in corotating interaction regions at 1 AU: Evidence for statistical ion acceleration, *Planet. Space Sci.*, *33*, 557-569, 1985.
- Ruzmaikin, A.A., J. Feynman, B.E. Goldstein, and E.J. Smith, Intermittent turbulence in solar wind from the south polar hole, *J. Geophys. Res.*, *100*, 3395-3403, 1995.
- Siscoe, G.L., and D.S. Intriligator, Macroscale coherence of

the heliospheric current sheet: Pioneer 10 and 11 comparisons, *Geophys. Res. Lett.*, *21*, 2075-2078, 1994.

Tsurutani, B.T., E.J. Smith, K.R. Pyle, and J.A. Simpson, Energetic protons accelerated at corotating shocks: Pioneer 10 and 11 observations from 1 to 6 AU, *J. Geophys. Res.*, *87*, 7389-7404, 1982.

---

D. S. Intriligator and G. L. Siscoe, Space Plasma Laboratory, Carmel Research Center, P.O. Box 1732, Santa Monica, CA 90406. (e-mail: /c=US/ADMD=telemail/S=Intriligator/G=Devrie/@x400.MSFC.NASA.gov; Siscoe@buasta.bu.edu)

(Received April 26, 1995; revised June 19, 1995; accepted June 19, 1995.)